

The unpublished Baško Polje (1971) lecture notes about two-dimensional NMR spectroscopy

J. Jeener

Faculté des Sciences (CPI-232), Campus Plaine, Université Libre de Bruxelles,
B-1050 Brussels, Belgium

Abstract. — The main part of this paper is a reproduction of (previously unpublished) lecture notes, which were circulated in 1971, and which are often cited as the initiation of two-dimensional NMR spectroscopy. A brief discussion follows, about the way of handling dates and durations in time-dependent quantum mechanics, and about the use of diagrams in NMR pulse spectroscopy in the usual or the superoperator formalisms.

I. Introductory remarks (1993).

The usual reference for the initiation of "two-dimensional" NMR spectroscopy refers to a talk which I gave at the AMPERE Summer School in Baško Polje (Yugoslavia) in September of 1971, and to unpublished notes written shortly after this meeting. It is a great pleasure to present these notes here (in section II), together with comments about the use of diagrams in pulsed high-resolution NMR (in section III), as a tribute to my professor, colleague and dear friend Anatole Abragam.

In 1971, many experiments had already been performed, in which the spin response was studied after a sequence of two (or more) pulses, with the variable separation between these pulses as an essential parameter. Well known examples of this procedure are the observation of the J-coupling in liquids by Hahn and Maxwell [1] and the manipulation of dipolar order by pulse techniques in solids [2]. I still remember searching for a long time, without success, for a pulse technique which would give results of the type presently given by NOESY, and ending up, almost in despair, with the COSY-like proposal of 1971. An important coworker in these efforts was Gerrit Alewaeters [3, 4]. Clearly, similar dreams developed in the minds of many people at that time, and a short conversation was often enough to convey the complete contents of the 1971 notes.

Very soon, it became clear that the idea had been presented for a very particular case, and also that it was not easy to turn into an efficient, practical tool. It has been very exciting for me to watch (and participate in) the impressive flourishing of theoretical

and experimental imagination which eventually made the success of 2D spectroscopy and its variants (see, for instance the book by Ernst, Bodenhausen and Wokaun [5]).

(Beginning of the 1971 lecture notes)

II. Pulse pair technique in high resolution NMR (1971).

by J. Jeener and G. Alewaeters

Faculty of Sciences, University of Brussels (ULB and VUB), Brussels, Belgium

(Preliminary manuscript, incomplete, November 14, 1971)

II.1 INTRODUCTION.

The usual CW and one-pulse Fourier transform methods of high-resolution NMR in liquids only provide very incomplete information about the nuclear spin Hamiltonian in the case of coupled spins. Additional information has been obtained by performing the measurements for different values of the external magnetic field, and by double resonance techniques. Essentially the same additional information about the nuclear spin Hamiltonian can also be obtained by the new technique proposed here.

A first r.f. pulse (90°) is applied at time $t = 0$ to the spin system in thermal equilibrium with the lattice. At time $t = t_1$, a second r.f. pulse (90° or 180°), coherent with the first pulse is applied and the transient nuclear magnetization is then measured as a function of the time t_2 elapsed since this second pulse. A large number of such measurements are performed for different values of t_1 . A double Fourier transform is then performed on these values, with respect to the variable t_1 (frequency ω_1) and to the variable t_2 (frequency ω_2). A theoretical discussion shows that inspection of this double Fourier transform immediately reveals which lines of the ordinary absorption spectrum do or do not belong to the same group of coupled spins, and that more detailed and quantitative information can be obtained easily. This technique should provide the same favorable signal-to-noise ratio as ordinary Fourier transform spectroscopy, and the quantitative interpretation of its results is simpler than that of double resonance techniques.

II.2 DENSITY MATRIX CALCULATIONS.

(in the case of a single kind of nuclear spins, neglecting spin-spin and spin-lattice relaxation)

In this section, we shall focus our attention on the spins in a single molecule.

II.2.1 *Spin Hamiltonian.*

In the case of a single magnetic ingredient, we can write the time-averaged spin Hamiltonian for one molecule of the liquid in the form

$$H = H_0 + H_{ss} (+H_{rf}) \quad (1)$$

where $H_0 = \hbar\omega_0 I_z$; ω_0 is an arbitrarily chosen frequency, in the neighborhood of the NMR frequency of the relevant nuclei (in practice, it is convenient to call ω_0 the frequency of the master oscillator of the pulse spectrometer); I_z is the component of \mathbf{I} in the direction of the large constant external magnetic field (the z -direction); \mathbf{I} is the sum of the spin operators for all the spins in the molecule; H_{ss} describes the chemical shifts of the various spins, the spin-spin couplings, and a term which compensates for the arbitrary choice of ω_0 ; and H_{rf} describes the effects of the pulses of resonant transverse rf magnetic field applied to the spin system.

As H_{ss} is very much smaller than H_0 in the present case, the effects which we shall be interested in can be discussed by means of the first order approximation eigenvalues of $H_0 + H_{ss}$ and of the corresponding zeroth-order eigenfunctions. These approximations are equivalent to replacing H_{ss} in the spin Hamiltonian (1) by the part H' of H_{ss} , which commutes with H_0 , so that the approximate spin Hamiltonian can be written as

$$H = H_0 + H' (+H_{rf}). \quad (2)$$

H_0 and H' are diagonalized simultaneously by the eigenstates $|a\rangle$ which we shall use later on:

$$\begin{aligned} H_0|a\rangle &= M_a \hbar\omega_0 |a\rangle \\ H'|a\rangle &= \hbar\omega_a |a\rangle. \end{aligned} \quad (3)$$

M_a is an integer (or a half-integer in the case of an odd number of half-integer spins), and a is just a label which completely specifies one eigenstate.

II.2.2 Rotating frame.

For simplicity, we shall discuss the dynamical behavior of the spin system in a frame of reference which rotates around the direction of the external magnetic field at the angular velocity ω_0 (approximately the NMR frequency of the spins). The components of any vector \mathbf{B} along the X and Y directions of the rotating frame will be denoted by \bar{B}_X and \bar{B}_Y . Every operator A in the laboratory frame can be described in the rotating frame by an operator \hat{A} given by

$$\hat{A} = V^\dagger A V, \text{ where } V = \exp(-i\omega_0 t I_z). \quad (4)$$

In the approximation (2), the equation of motion for the density operator can be written as

$$i\hbar \frac{\partial}{\partial t} \hat{\rho}(t) = \left[\left\{ H' + \hat{H}_{rf} \right\}, \hat{\rho}(t) \right]. \quad (5)$$

In the absence of rf irradiation, the formal solution of this equation is

$$\hat{\rho}(\tau + t) = Q(t) \hat{\rho}(\tau) Q^\dagger(t) \text{ where } Q(t) = \exp\{-(it/\hbar)H'\}. \quad (6)$$

The effects of a short, intense, pulse of resonant rf magnetic field on the density matrix can be described, in the rotating frame, by the finite rotation operator

$$R(\theta, \phi) = \exp\{-i\theta(I_X \cos \phi + I_Y \sin \phi)\}, \quad (7)$$

where θ is the magnitude of the pulse and ϕ its phase. The spin property which is usually measured experimentally is one of the transverse components of the average spin magnetization in the laboratory frame, for instance $\langle I_x \rangle$. This quantity can be expressed in terms of the X and Y components of the spin magnetization in the rotating frame as

$$\langle I_x \rangle = \langle \bar{I}_X \rangle \cos \omega_0 t + \langle \bar{I}_Y \rangle \sin \omega_0 t = \text{real part of } \{ \langle \bar{I}_+ \rangle \exp(i\omega_0 t) \}, \quad (8)$$

where $\langle \bar{I}_+ \rangle = \langle \bar{I}_X \rangle + i \langle \bar{I}_Y \rangle = \text{Tr} \{ I_+ \hat{\rho} \}$. It is clear from this expression that the nuclear induction signals originating from $\langle \bar{I}_X \rangle$ and $\langle \bar{I}_Y \rangle$ have orthogonal rf phases, and that these two quantities can be measured simultaneously by the use of a coherent instrumentation with two orthogonal phase sensitive detectors. The trace calculations which follow can be somewhat simplified by the introduction of the quantity $\langle \bar{I}_+ \rangle$ instead of $\langle \bar{I}_X \rangle$ and $\langle \bar{I}_Y \rangle$.

II.2.3 Single pulse experiments.

As a preparation for the discussion of the two-pulse experiments, let us first use the same techniques and notations in the well-known case of single pulse "Fourier spectroscopy".

We shall always assume that the spin system has reached complete thermal equilibrium with the lattice before each experiment. In the standard high temperature approximation, the corresponding equilibrium density matrix can be written as

$$\rho_{\text{eq}} = \hat{\rho}_{\text{eq}} = \frac{1}{Z} \left\{ 1 - \frac{\hbar\omega_0}{kT} I_z \right\}, \quad (9)$$

where T is the lattice temperature and Z is a normalization constant.

Let us now apply to the spin system a 90° pulse oriented in the Y direction of the rotating frame. This pulse will rotate the spin magnetization from the z direction to the X direction and the density matrix immediately after the pulse, $\hat{\rho}(0_+)$, can be written as

$$\hat{\rho}(0_+) = \frac{1}{Z} \left\{ 1 - \frac{\hbar\omega_0}{kT} \bar{I}_X \right\} = \frac{1}{Z} - \alpha (\bar{I}_+ + \bar{I}_-), \quad (10)$$

where $\alpha = \hbar\omega_0/2kTZ$ and $\bar{I}_\pm = \bar{I}_X \pm \bar{I}_Y$. At a time t_1 after the pulse, the density matrix will be given by

$$\hat{\rho}(t_1) = \frac{1}{Z} - \alpha Q(t_1) \{ \bar{I}_+ + \bar{I}_- \} Q^\dagger(t_1), \quad (11)$$

and the measurable quantities can be summarized as

$$\langle \bar{I}_+ \rangle = -\alpha \text{Tr} \{ I_+ Q(t_1) \{ \bar{I}_+ + \bar{I}_- \} Q^\dagger(t_1) \}. \quad (12)$$

Expression (12) for $\langle \bar{I}_+ \rangle$ can be easily written under the more familiar form (13) by performing the following steps:

1) evaluate the trace as a sum of diagonal matrix elements in the representation defined by (3),

2) note that $Q(t_1)$ is diagonal in this representation and that $\langle a | Q(t_1) | a \rangle = \exp(-i\omega_a t_1)$,

3) note that $\langle a|\bar{I}_+|b\rangle$ can be different from zero only if $M_a = M_b + 1$.

$$\begin{aligned}\langle \bar{I}_+ \rangle &= -\alpha \sum_{a,b} \langle a|\bar{I}_+|b\rangle e^{-i\omega_b t_1} \langle b|\bar{I}_-|a\rangle e^{i\omega_a t_1} \\ &= -\alpha \sum_{a,b} |\langle a|\bar{I}_+|b\rangle|^2 e^{i(\omega_a - \omega_b)t_1}.\end{aligned}\quad (13)$$

This expression shows that the Fourier transform of $\langle \bar{I}_+ \rangle$ after one pulse consists, as is well known, of one line at each of the NMR frequencies $(\omega_a - \omega_b)$ of the spin system, the intensity of each line being proportional to the corresponding value of $|\langle a|\bar{I}_+|b\rangle|^2$. The quantities $(\omega_a - \omega_b)$ are the rotating frame NMR frequencies, which are related to the usual laboratory frame NMR frequencies by the obvious equation $\omega_{(\text{NMR, lab.frame})} = \omega_0 + \omega_{(\text{NMR, rot.frame})}$.

II.2.4 Two pulse experiments.

Each two-pulse experiment begins in the same way as the one-pulse experiment described above. At time t_1 , a second pulse, described by the finite rotation operator R , is applied to the spin system. At time $t_1 + t_2$, which means t_2 after the second pulse, the density matrix will be given by

$$\hat{\rho}(t_1 + t_2) = \frac{1}{Z} - \alpha Q(t_2) R Q(t_1) \{ \bar{I}_+ + \bar{I}_- \} Q^\dagger(t_1) R^\dagger Q^\dagger(t_2), \quad (14)$$

and the transverse magnetization by

$$\langle \bar{I}_+ \rangle = -\alpha \text{Tr} \{ \bar{I}_+ Q(t_2) R Q(t_1) \{ \bar{I}_+ + \bar{I}_- \} Q^\dagger(t_1) R^\dagger Q^\dagger(t_2) \}. \quad (15)$$

Using the steps which lead from (12) to (13), we can rewrite (15) under the following, more usable, form of a double Fourier transform of $\langle \bar{I}_+ \rangle$ with respect to the two independent time variables t_1 and t_2 :

$$\begin{aligned}\langle \bar{I}_+ \rangle &= -\alpha \sum_{a,b,c,d} \langle a|\bar{I}_+|b\rangle \langle b|R|d\rangle \langle d|\bar{I}_-|c\rangle \langle c|R^\dagger|a\rangle e^{i(\omega_c - \omega_d)t_1} e^{i(\omega_a - \omega_b)t_2} \\ &\quad -\alpha \sum_{a,b,c,d} \langle a|\bar{I}_+|b\rangle \langle b|R|c\rangle \langle c|\bar{I}_+|d\rangle \langle d|R^\dagger|a\rangle e^{-i(\omega_c - \omega_d)t_1} e^{i(\omega_a - \omega_b)t_2}.\end{aligned}\quad (16)$$

Figure 1 provides a diagram-like representation of one non-zero term of the first summation in (16) and one non-zero term of the second summation.

Let us denote by ω_1 the frequency which is associated with t_1 in this double Fourier transform, and ω_2 that associated with t_2 . The presence of matrix elements of \bar{I}_+ and \bar{I}_- in (16) immediately shows that the double Fourier transform of $\langle \bar{I}_+ \rangle$ at ω_1 and ω_2 can be different from zero only if ω_2 is one of the NMR frequencies of the spin system and ω_1 is either one of these frequencies (first term in the rhs of (16)) or minus one of these (second term of the rhs of (16)).

The absolute value of the relevant matrix elements of \bar{I}_+ and \bar{I}_- can be obtained experimentally from the ordinary NMR absorption spectrum, so that a complete set of

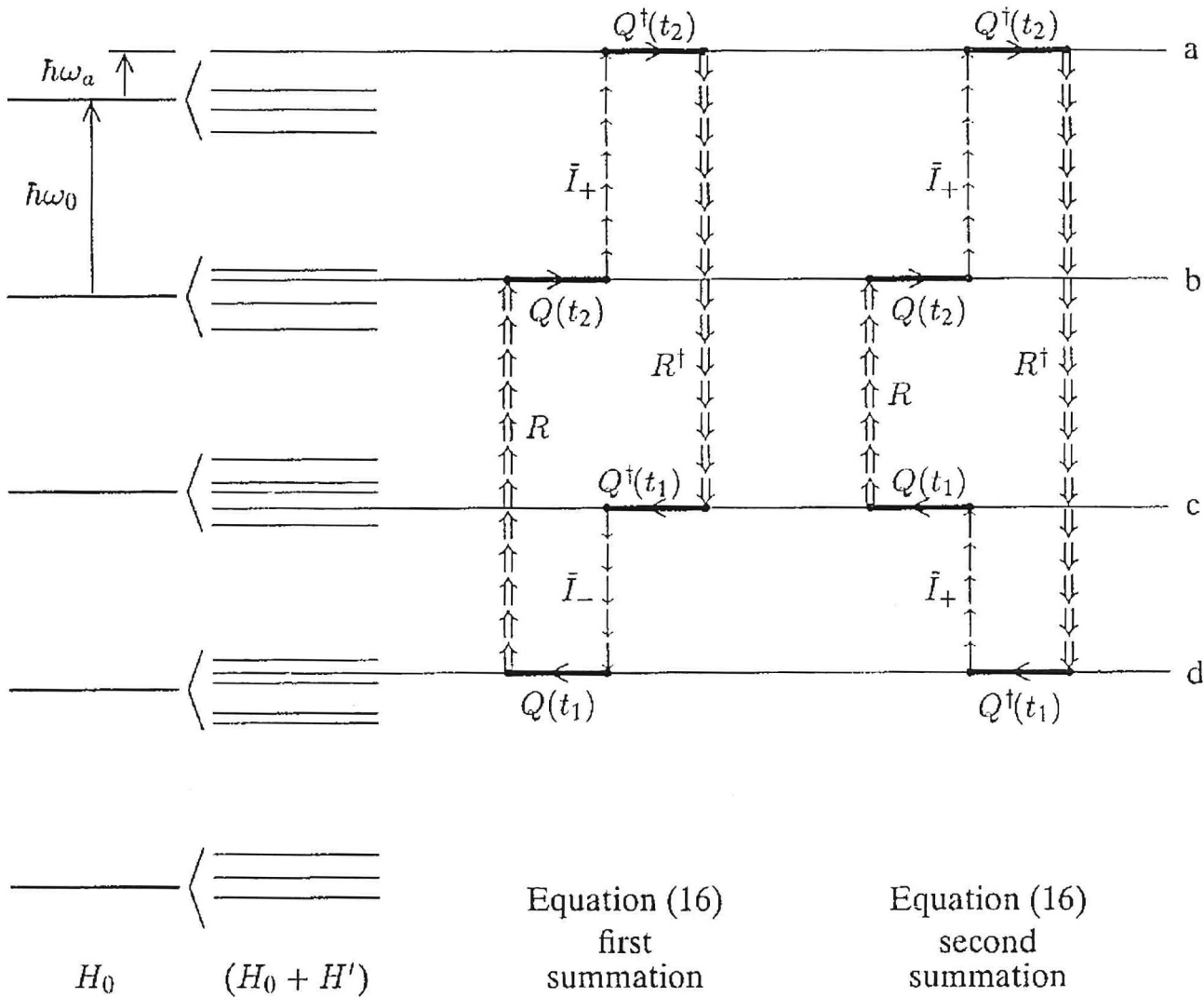


Fig. 1. — Diagram representation of one non-zero term in each of the two summations in equation (16). The direction around the loops corresponds to reading equation (16) from right to left.

two-pulse experiments, followed by a double Fourier transform, provides a lot of direct information about the matrix elements of the finite rotation operator R and thus, also, about the spin Hamiltonian. One should note, in this connection, that it is quite frequent that a number of different transitions in a molecule do contribute to the same NMR line. Whenever this happens, the quantities actually measured are of course the sums of all the terms in (16) which correspond to given values of ω_1 and ω_2 . One should also note that the finite rotation operators R do have less restrictive selection rules than \bar{I}_+ and \bar{I}_- : for instance, if two eigenstates can be individually connected by a chain of non-zero matrix elements of \bar{I}_+ and \bar{I}_- , they are in general directly connected by a non-zero matrix element of R .

Let us now imagine that the liquid under consideration contains different kinds of molecules. The ordinary NMR spectrum will, then, be the superposition of the spectra of each of the molecular species, and the response in a two pulse experiment will also be the superposition of the responses of each species. In particular, the double Fourier

transform of $\langle \tilde{I}_+ \rangle$ will contain *no* non-zero terms for which ω_1 (or $-\omega_1$) and ω_2 correspond to NMR frequencies of different molecules. As a consequence of this remark, the existence of a non-zero term in a double Fourier transform of $\langle \tilde{I}_+ \rangle$ implies that the two relevant NMR frequencies do belong to the same molecule.

If the spins in a molecule can be sorted out in two different groups, such that no spin in one group is coupled to any spin in the other group, then the two spin groups will in fact behave as though they belonged to different molecules. The above discussion then shows that the existence of a non-zero term in a double Fourier transform of $\langle \tilde{I}_+ \rangle$ implies that the two relevant frequencies belong to the same group of coupled spins. In this way, the two-pulse technique can be used as an alternative to double resonance in the sorting out of NMR lines in families.

II.3 MISCELLANEOUS NOTES.

II.3.1 *General organization of an experiment.*

After each two-pulse sequence, the nuclear induction signal must be recorded as a function of t_2 after the second pulse; a large number of such two-pulse sequences must be studied in order to examine the influence of the time separation t_1 between the two pulses; the double Fourier transform must be evaluated, displayed, understood.

All this seems to imply the manipulation, storage, ..., of a prohibitively large quantity of information. One possible way of actually performing the experiment would be the following:

- (a) after each two-pulse sequence, one computes the Fourier transform of the nuclear induction signal at a few well chosen NMR frequencies ω_2 , and these results are stored on tape, together with the corresponding value of t_1 ,
- (b) this procedure is repeated for a large number of values of t_1 , storing all the results on tape,
- (c) the tape is read, and a complete Fourier transform in ω_1 is computed for each of the chosen values of ω_2 .

II.3.2 *Sensitivity of the method.*

Let us focus our attention on two NMR lines, at $(\omega_a - \omega_b)$ and $(\omega_c - \omega_d)$, which we shall assume to be of equal intensities and to originate each from a single transition in the spin system. A comparison of expressions (13) and (16) then shows that the double Fourier transform at $(\omega_a - \omega_b)$ and $(\omega_c - \omega_d)$ is smaller than the single Fourier transform at each of these frequencies by a factor $\langle b|R|d \rangle \langle c|R^\dagger|a \rangle$ which is, roughly speaking, of order $1/N$, where N is the number of eigenstates of the relevant group of coupled spins which can be reached from $|a\rangle$ by means of the operator R . In many interesting cases, N is not larger than 10.

The factor $\langle b|R|d \rangle \langle c|R^\dagger|a \rangle$ is also roughly the ratio of signal-to-noise ratios which can be achieved in a same length of time for the detection of the peaks in the double Fourier transform and in the single Fourier transform.

II.3.3 Some other advantages of the double pulse method.

- Very simple theory (no rf ON, except for two short pulses).
- No role played by spin-lattice relaxation, Overhauser effect, ...
- No special problem in the case of two close-by lines.
- Direct *quantitative* information about the matrix elements of R .
- Lots of information gathered in a single run.
- Possibility of correcting for frequency or phase drift during the run, by software.

(End of the 1971 lecture notes)

III. Improved diagram representations (1993).

I have found diagrams of the type shown in Figure 1 very convenient to visualize the structure of the various contributions to 2D and n D spectra, and also in attempts to devise new pulse sequences generating such spectra. However, the improvements described in the following subsections make these diagrams more readable, hence more useful.

III.1 EMPHASIZING THE ROLE OF TIME (i.e. DATE).

The closed loop structure of the diagrams in Figure 1 was meant to display the cyclic property of equation (16) as far as states are concerned: reading from right to left, for instance, one starts in state a , goes through states b , c and d , and eventually comes back to state a . This situation is more explicitly shown by the following intermediate between equations (15) and (16):

$$\begin{aligned}
 \langle \bar{I}_+ \rangle = & \\
 -\alpha \sum_{a,b,c,d} & \langle a | I_+ | b \rangle \langle b | Q(t_2) | b \rangle \langle b | R | d \rangle \langle d | Q(t_1) | d \rangle \langle d | I_- | c \rangle \langle c | Q^\dagger(t_1) | c \rangle \langle c | R^\dagger | a \rangle \langle a | Q^\dagger(t_2) | a \rangle \\
 & + \text{second term in equation (25).}
 \end{aligned} \tag{17}$$

Equations of types (15), (16) or (17) are also cyclic in time or, more exactly, in *date*: reading the first term in the r.h.s. of equation (17) from right to left, one starts at the date of the measurement, goes back in steps to the date immediately after the first pulse (where the relevant part of ρ is I_-), then proceeds forward in steps, eventually coming back to the date of measurement of $\langle \bar{I}_+ \rangle$.

Discussions in which dates play an essential role will be clarified by the introduction of an appropriate notation. In the present paper, we shall denote dates by the greek letter τ , and durations by the latin letter t (in both cases with indices as needed). Evolution operators will be written as $U(\tau_2, \tau_1)$, with the usual property $|\psi(\tau_2)\rangle = U(\tau_2, \tau_1)|\psi(\tau_1)\rangle$, and the relations with the notation of the 1971 notes (Eq. (6)) are

$$Q(t) \rightarrow \hat{U}(\tau+t, \tau) \quad \text{and} \quad Q^\dagger(t) \rightarrow \hat{U}(\tau, \tau+t) \quad \text{for any } \tau, \tag{18}$$

where the interaction representation version of $U(\tau_2, \tau_1)$ is given by ⁽¹⁾ (see Eq. (4))

$$\hat{U}(\tau_2, \tau_1) = V^\dagger(\tau_2) U(\tau_2, \tau_1) V(\tau_1). \quad (19)$$

The rotation operator R (Eq. (7)), describing the effects of a short rf pulse applied at date τ , will also be written as an evolution operator acting between dates τ_- and τ_+ (respectively immediately before and after the pulse), and the relations with the notation of the 1971 notes (Eq. (7)) are

$$R \rightarrow \hat{R}(\tau_+, \tau_-) \quad \text{and} \quad R^\dagger \rightarrow \hat{R}(\tau_-, \tau_+). \quad (20)$$

With these changes in notation, also denoting by τ_0 (instead of 0) the date of the first 90° pulse, equation (17) takes the form

$$\begin{aligned} \langle \hat{I}_+ \rangle = & -\alpha \sum_{a,b,c,d} \langle a | I_+ | b \rangle \langle b | \hat{U}(t_2+t_1+\tau_0, t_1+\tau_0+) | b \rangle \langle b | \hat{R}(t_1+\tau_0+, t_1+\tau_0-) | d \rangle \langle d | \hat{U}(t_1+\tau_0-, \tau_0+) | d \rangle \\ & \times \langle d | I_- | c \rangle \langle c | \hat{U}(\tau_0+, t_1+\tau_0-) | c \rangle \langle c | \hat{R}(t_1+\tau_0-, t_1+\tau_0+) | a \rangle \langle a | \hat{U}(t_1+\tau_0+, t_2+t_1+\tau_0) | a \rangle \\ & + \text{second term in equation (16)}. \end{aligned} \quad (21)$$

The left part of Figure 2 provides a diagram-like representation of one non-zero term of the summation displayed in equation (21), with the date explicitly shown as the horizontal coordinate. This type of diagram makes the detailed date and state structure obvious, and emphasizes the fact that, in each term of the sum, each evolution operator (of type \hat{U} or \hat{R}) appears *twice* with opposite order of the date arguments. Of course, the two occurrences of one same operator do not describe independent transformations, hence the redundancy is undesirable for the sake of clarity, and one is tempted to lump the offenders together as suggested by the diagram in the right part of Figure 2. One of the many advantages of the "Liouville space" or "super-operator" presentation of quantum mechanics is to provide a simple and natural way of achieving this goal.

III.2 USING A SUPERKET-SUPERBRA-SUPEROPERATOR FORMALISM.

III.2.1 *Brief summary about superoperators.*

Details about the point of view and notation used here can be found, for instance, in references [5] and [6].

To each linear operator A (in practice, density operator or observable), we associate a superket $|A\rangle_s$, where a non-traditional subscript s is used here to distinguish superkets from standard kets. To each linear operator B , we also associate a superbra $\langle B|_s$, using the trace metric and requiring that

$$\langle B|_s A \rangle = \text{Tr}(B^\dagger A) \quad \text{for every operator } A. \quad (22)$$

⁽¹⁾ In reference [6], the role of V is played by an evolution operator involving *two* dates. I feel that this was an unfortunate choice, and that a unitary operator involving a single date should be used, as explained in references [7] and [8](appendix D).

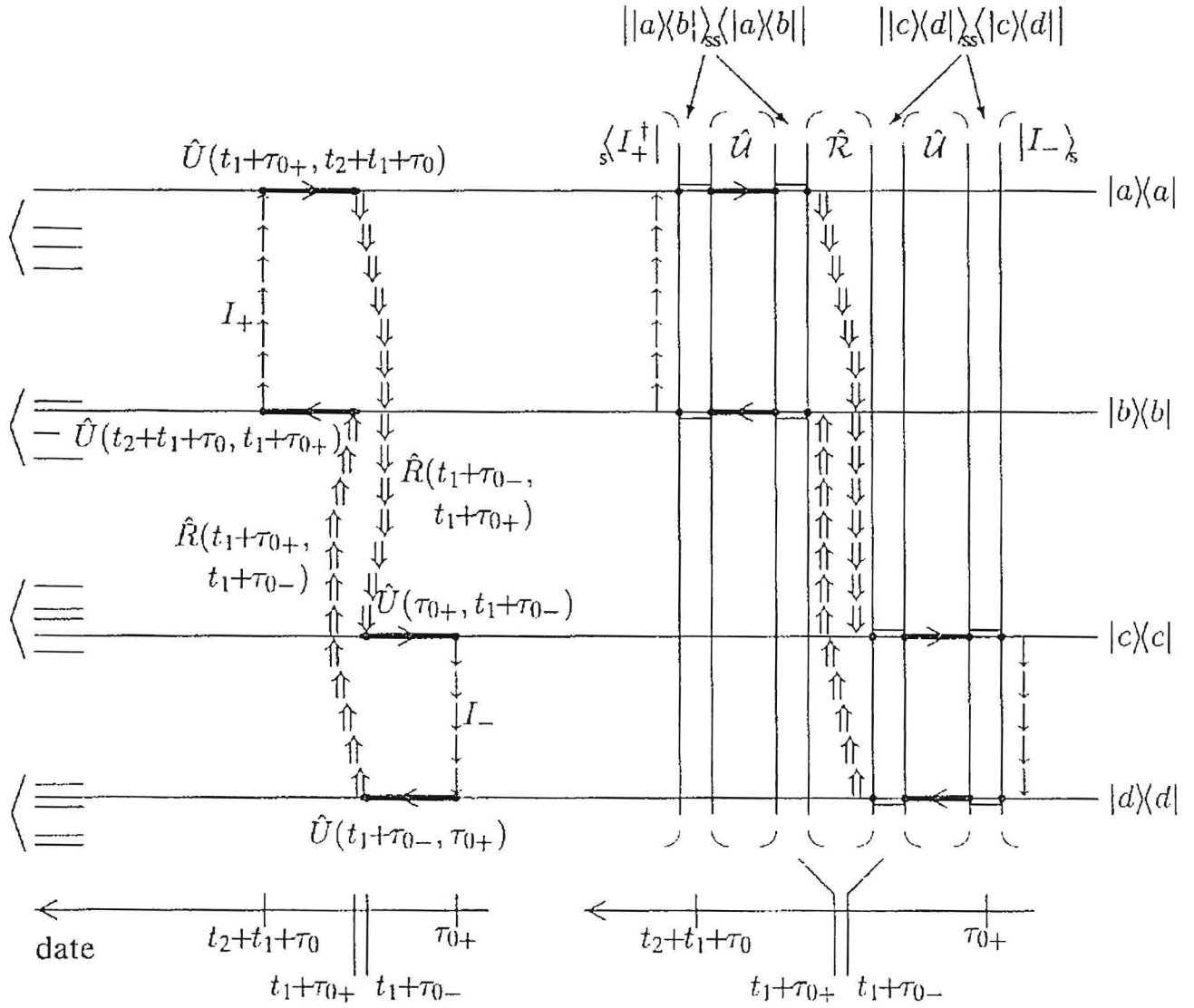


Fig. 2. — Improved diagram representations of one non-zero term in the first summation in equation (16). The horizontal coordinate now corresponds to time (i.e. date), running from right to left to match the usual typography. The diagram on the left is for the usual ket-bra-operator formalism, the direction around the loop still corresponds to reading equations (16) or (21) from right to left. The relation between the ordering of states and dates in this diagram and in equation (21) is the following: $\langle e | \hat{U}(\tau_2, \tau_1) | f \rangle$ is represented in the diagram by a segment along which one goes from f towards e and from τ_1 towards τ_2 when moving in the direction shown by the arrow(s) (irrespective of whether τ_1 is earlier or later than τ_2). The same convention holds for the operators \hat{R} . With this convention, it is no longer necessary to explicitly indicate the date arguments of the operators in the diagram. The right part of the figure suggests a way of grouping the two versions of each evolution operator corresponding to the same pair of dates, and gives hints about the corresponding superoperator notation (see also Fig. 3).

Linear transformations of superkets will be described as superoperators, and denoted here by script symbols, e.g. \mathcal{U} , \mathcal{R} or \mathcal{L} , with the exception of the unit superoperator 1_s . The action of a superoperator on a superbra is defined by requiring that $\langle A | \mathcal{G} | B \rangle_s = (\langle A | \mathcal{G}) | B \rangle_s = \langle A | (\mathcal{G} | B \rangle_s)$ for any A and B .

The set of superkets $\{|A_i\rangle_s\}$ is a basis (in superket space) if it satisfies the orthonormality and closure relations, respectively

$${}_s\langle A_i | A_j \rangle_s = \delta_{i,j} \quad \text{and} \quad \sum_i |A_i\rangle_s \langle A_i| = 1_s. \quad (23)$$

An important particular type of transformation of operators consists in taking any operator B in a sandwich between operators A and C , leading to the new operator $F = ABC$. The superoperator counterpart of this can be written as

$$|F\rangle_s = |ABC\rangle_s = \mathcal{D}|B\rangle_s \quad \text{where} \quad \mathcal{D} = A \times C, \quad (24)$$

where the *decomposable* superoperator \mathcal{D} is *composed* of the operators A and C .

With this notation, the usual Von Neumann equation of motion $i\hbar \partial \rho(\tau) / \partial \tau = [H(\tau), \rho(\tau)]$ can be written as

$$i\hbar \frac{\partial}{\partial \tau} |\rho(\tau)\rangle_s = \mathcal{L}(\tau) |\rho(\tau)\rangle_s \quad \text{where} \quad \mathcal{L}(\tau) = (H(\tau) \times 1_s) - (1_s \times H(\tau)), \quad (25)$$

where $\mathcal{L}(\tau)$ is called the Liouvillian. The interaction representation transformation (4) now takes the form

$$|\hat{A}(\tau)\rangle_s = \mathcal{V}^\dagger(\tau) |A(\tau)\rangle_s, \quad \text{where} \quad \mathcal{V}(\tau) = V(\tau) \times V^\dagger(\tau) \quad (26)$$

and $V(\tau) = \exp(-i\omega_0 \tau I_z)$, and the motion in the absence of rf irradiation is described by obvious extensions of (6) and (19):

$$|\rho(\tau_2)\rangle_s = \mathcal{U}(\tau_2, \tau_1) |\rho(\tau_1)\rangle_s \quad \text{where} \quad \mathcal{U}(\tau_2, \tau_1) = U(\tau_2, \tau_1) \times U(\tau_1, \tau_2). \quad (27)$$

Using a similar notation for the rotation operators, we can write expression (15) for $\langle \bar{I}_+ \rangle$ under the form

$$\langle \bar{I}_+ \rangle = -\alpha {}_s\langle \bar{I}_+^\dagger | \hat{\mathcal{U}}(t_2+t_1+\tau_0, t_1+\tau_0+) \hat{\mathcal{R}}(t_1+\tau_0+, t_1+\tau_0-) \hat{\mathcal{U}}(t_1+\tau_0-, \tau_0+) | (\bar{I}_+ + \bar{I}_-) \rangle_s, \quad (28)$$

where the date now increases systematically towards the future when the formula is read from right to left, and the evolution during each time interval is completely described by a single superoperator.

III.2.2 Diagrams for superoperators.

The formal expression (28) can be evaluated by inserting closure relations (23) on both sides of each superoperator:

$$\begin{aligned} \langle \bar{I}_+ \rangle &= -\alpha \sum_{i,j,k,l} {}_s\langle \bar{I}_+^\dagger | A_i \rangle_s \langle A_i | \hat{\mathcal{U}}(t_2+t_1+\tau_0, t_1+\tau_0+) | A_j \rangle_s \langle A_j | \hat{\mathcal{R}}(t_1+\tau_0+, t_1+\tau_0-) | A_k \rangle_s \\ &\quad \times {}_s\langle A_k | \hat{\mathcal{U}}(t_1+\tau_0-, \tau_0+) | A_l \rangle_s \langle A_l | (\bar{I}_+ + \bar{I}_-) \rangle_s. \end{aligned} \quad (29)$$

If the basis superkets $|A_i\rangle_s$ are chosen to be eigensuperkets of the Liouvillian \mathcal{L} , they are also eigensuperkets of the evolution superoperator \mathcal{U} , hence the terms in (29) will differ

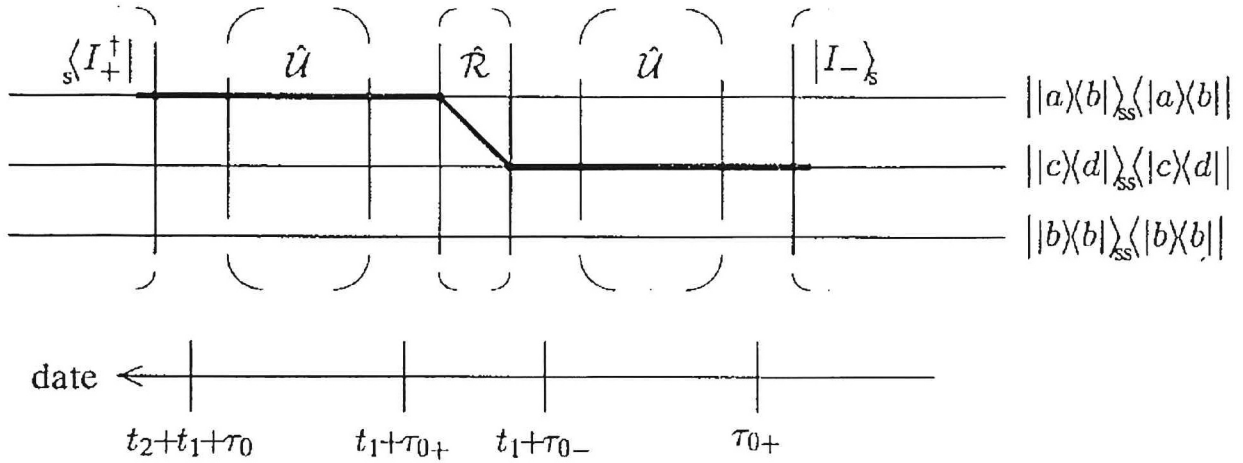


Fig. 3. — Superoperator diagrams. The notation is that of equation (29) in the particular case of a level-shift basis constructed with the eigenstates of the Hamiltonian. The horizontal lines are labeled by the superprojectors which appear in the closure relation (23) for superkets. The left-right ordering in these diagrams is exactly the same as the typographical order in equation (29). This figure shows the contribution to $\langle \hat{I}_+ \rangle$ for which the left part of Figure 2 gives an operator diagram.

from zero only if $i = j$ and $k = l$, considerably simplifying the expression. In the present case, a suitable basis (in superket space) can be constructed with the set of level-shift operators $\{|a\rangle\langle b|\}$ of the ket basis (3) which diagonalizes the Hamiltonian. The superket basis $\{||a\rangle\langle b||_s\}$ (for all a and b) diagonalizes the Liouvillian (25),

$$\mathcal{L}||a\rangle\langle b||_s = \hbar(\omega_a - \omega_b)||a\rangle\langle b||_s, \quad (30)$$

and the evolution superoperator \mathcal{U} ,

$$\mathcal{U}(\tau_2, \tau_1)||a\rangle\langle b||_s = e^{-i(\omega_a - \omega_b)(\tau_2 - \tau_1)}||a\rangle\langle b||_s, \quad (31)$$

as can be checked easily using the following general property of all superket bases constructed with level-shift operators (see for instance Ref. [6]):

$$\langle_s |a\rangle\langle b| (A \times B) |c\rangle\langle d| \rangle_s = \langle a |A| c \rangle \langle d |B| b \rangle. \quad (32)$$

One term of the summation (29), obtained with this superket basis, is shown in the top part of Figure 3 and in the right part of Figure 2. With the help of the figures and of the above expressions, one can easily verify the equivalence of expressions obtained with the ket-bra-... and with the superket-superbra-... formalisms for problems in which relaxation is ignored. As a further example of the use of superoperator diagrams, Figure 4 shows a more complete description of two-pulse experiments, in which the two pulses are treated explicitly and the initial condition is described in terms of populations of the eigenstates of the Hamiltonian.

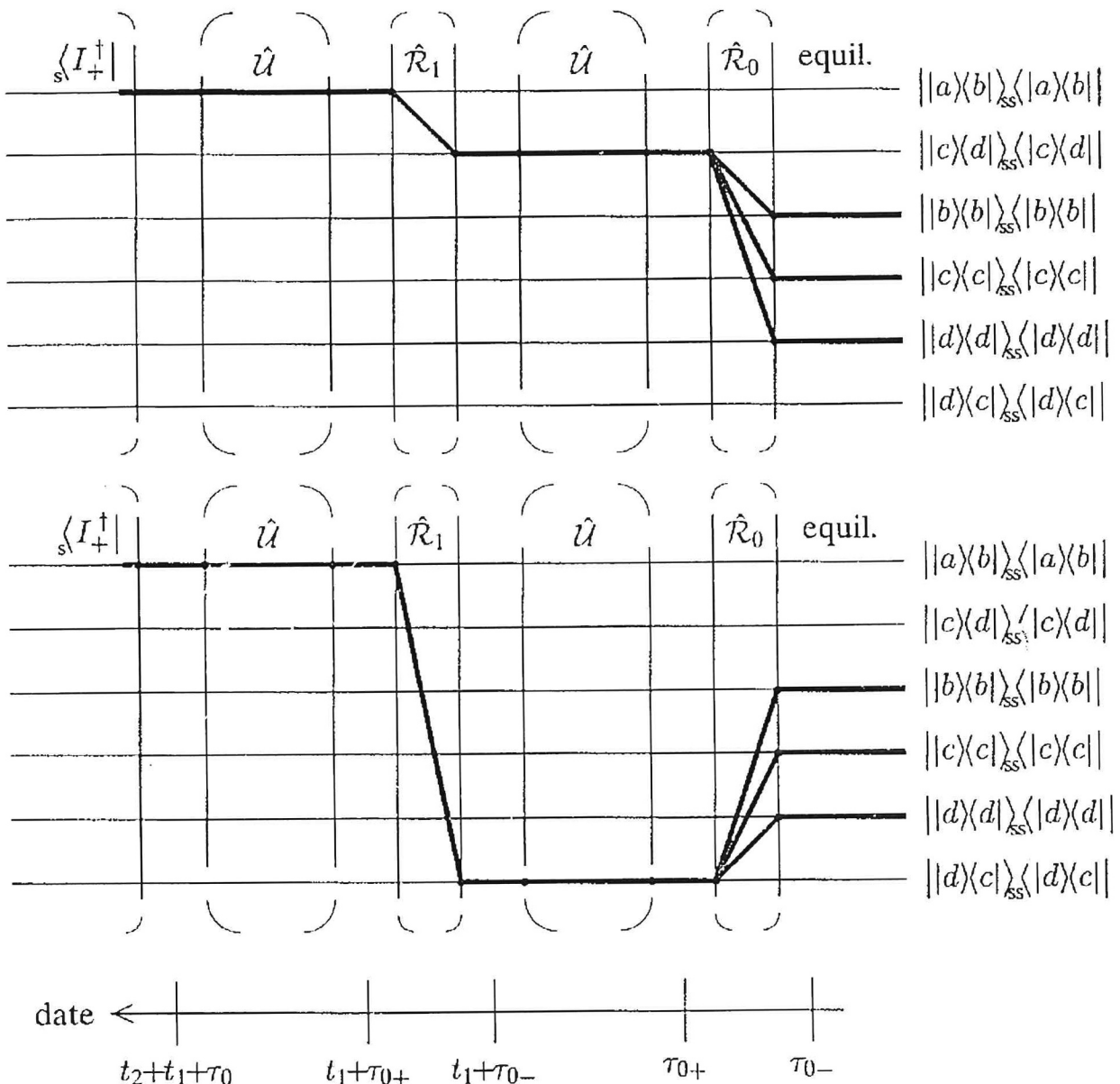


Fig. 4. — Superoperator diagrams drawn with the same conventions as in Figure 3. This figure gives a more complete representation of a two-pulse experiment, starting with thermal equilibrium for $\tau < \tau_{0-}$, and describing the two pulses \hat{R}_0 at date τ_0 and \hat{R}_1 at date $t_1 + \tau_0$. The diagrams show the contributions, arising from the equilibrium populations of the eigenstates b , c and d of the Hamiltonian, respectively to the left diagram of Figure 1 (top) and to the right diagram of Figure 1 (bottom).

However, in any attempt to take relaxation into account, the use of a superoperator formalism is not a matter of elegance or personal preference any more, but one of necessity. Under these circumstances, the convenient bases in superket space are usually *not* constructed from level shift operators, the corresponding expressions do not have simple equivalents in terms of kets, bras and operators, but superoperator diagrams can still be useful to organize and visualize the calculations.

References.

- [1] HAHN E. L., MAXWELL D. E., *Phys. Rev.* **88** (1952) 1070.
- [2] JEENER J., BROEKERT P., *Phys. Rev.* **157** (1967) 232.
- [3] ALEWAETERS G., Licentiaat Verhandeling, Vrije Universiteit Brussel (1969).
- [4] ALEWAETERS G., Thesis, Vrije Universiteit Brussel (1976).
- [5] ERNST R. R., BODENHAUSEN G., WOKAUN A., Principles of Nuclear Magnetic Resonance in One and Two Dimensions (Clarendon Press, 1987).
- [6] JEENER J., *Adv. Magn. Reson.* **10** (1982) 1.
- [7] JEENER J., *Bull. Magn. Reson.* **16** (1994) 42.
- [8] JEENER J., HENIN F., *Phys. Rev. A* **34** (1986) 4897.